



Optical Properties of PVA Silicon Carbide Nano Composites Films Synthesized Via Laser Ablation

Hamid Shaker Mohsen*¹, Hisham Mohammed Ali Hasan*²

¹* Department of Physics ,College of Education; edu-phy3.post@qu.edu.iq University of Al-Qadisiyah, Diwaniyah in Iraq

² Department of Physics ,College of Education; hisham.hasan@qu.edu.iq University of Al-Qadisiyah, Diwaniyah in Iraq

*Corresponding author email: hisham.hasan@qu.edu.iq

الخصائص البصرية لأغشية PVA كربيد السيليكون النانوية المركبة عن طريق الاستئصال بالليزر

حامد شاكر محسن*¹, هشام محمد علي حسن²

¹* قسم الفيزياء ، كلية التربية ، edu-phy3.post@qu.edu.iq ، جامعة القادسية ، الديوانية ، العراق

² قسم الفيزياء ، كلية التربية ، hisham.hasan@qu.edu.iq ، جامعة القادسية ، الديوانية ، العراق

Accepted:

13/7/2023

Published:

30 /9 /2023

Abstract

Background: Enhancing the optical characteristics of nano-silicon carbide and polyvinyl alcohol films is thought to be crucial for obtaining the semiconductor with the lowest energy gap for applications in electrical devices, digital displays, and sensors.

Materials and Methods: Poly vinyl alcohol and silicon carbide's optical properties were examined. A pulsed laser with a 532 nm wavelength is used to create these nanoparticles into widespread nanoparticles in two environments (water and vinyl alcohol). Polyvinyl alcohol nanocomposite was created by spin coating silicon carbide particles with the weight fractions 0.90%, 0.91%, 0.93%, and 0.95%. Fourier spectroscopy was used to locate the functional groups based. Techniques FESEM were used to analyze the surface composition and nanoparticle dispersion on the membrane-surface of the nanocomposite. using spectroscopy UV-Vis used to record the absorbance spectrum in the range of (200-800) nm for ultraviolet radiation.

Results: The direct energy gap (5.585, 5.310, 5.480, 4.986, 4.800) eV and the indirect (5.006, 4.880, 4.916, 4.683, 4.490) eV and Urbach energy (2.38, 2.45, 2.94, 2.74, 3.67) eV were calculated. for the samples by ratio, as shown in Table No. 1.

Conclusion: By investigating the optical characteristics of nanoparticles, such as their extinction and absorption coefficients, direct and indirect optical energy gaps, and Urbach energies .increase in extinction and absorption coefficients Urbach energy when adding nano carbide to polyvinyl alcohol, results show narrowing of the direct and indirect energy gaps. This suggests that the nanocomposite's optical characteristics have improved.

Keywords: Nanocomposites, PVA, SiC, UV-VIS, FTIR.



1. INTRODUCTION

Due to their widespread application in several industries, including photovoltaics, polymer composites—polymers plus additives—are the material of choice. [1], optoelectronics [2], preserving energy [3], supercapacitors [4], suppresses the flames [5], sensors [6], etc. are used in optical waveguide materials, colorimetric materials, solar cells, and light-emitting diodes (LEDs) as both passive and active layers [7]. In this regard, materials for photovoltaics are preferred due to their low cost and energy consumption. But the production process has grown increasingly challenging [8]. In previous research [9], Severe nanoparticles were sensitive to aggregating around PVA during the nanoparticles' dispersion in the PVA matrix. The tendency of the crystals to form blocs as a result of Vandrfal's forces and the insufficient adhesion between the PVA matrix as reinforcing material are the main causes of this, To achieve stability and the uniform dispersion of SiC nanocrystals in the polymer matrix, focused study has been conducted in this regard. JS Cao et al, the presented a technique for coating the surface of SiC nanocrystals with polystyrene to increase the interfacial adhesion between a polymer matrix and SiC nanocrystals [10]. In the current study, SiC nanocrystals were used to improve their dispersion in a PVA matrix using distilled non-ionic water [11]. Utilizing FTIR research, the functionalization of SiC nanocrystals was validated, and the impact of SiC nanocrystals on the optical characteristics of PVA was thoroughly examined [12].

2. EXPERIMENTAL SECTION.

2.1. Materials

For the ablation of nanoscale silicon carbide, coarse silicon carbide No. 800 was employed as a laser target, and distilled deionized water (DW) was required to prepare all samples. Both NPs and a polymer solution have been produced using it in laser ablation. Approximately (7) and (5 106) /cm of water and resistivity (PH) were measured, respectively. The current work made use of polyvinyl alcohol (PVA).

2.2 Nanostructure

Nano silicon carbide was prepared by laser ablation with a pulse wavelength of 532 nm, energy of 200 mJ, frequency of 6 Hz, and pulse rate, by placing the carbide piece in deionized distilled water in a beaker, and the piece is placed in the distance equal to the focal length of the lens It is 10 cm. In the concentration and extraction of sic NP, an amount of polyvinyl alcohol with different masses was prepared, whose mass was measured with a 6-level sensitive scale, and then mixed with a magnetic stirrer, the proportions of sample No. 1 (0.8 g of PVA 100 wt%, sic = 0 wt%) and sample #2 (0.79 g of PV = 99.10 wt%, sic = 0.90 wt%), sample #3 (0.78 g of PVA = 99.09 wt%, sic = 0.91 wt%), sample #4 (0.77 g of PVA = 99.07 wt% sic = 0.93 wt%) and sample #5 (0, 76 g of PVA = 99.05 wt%, sic = 0.95 wt%) as Table (1) shows. glass substrate with a circular shape, a diameter of 40 mm, and a thickness of 250 to 300 m was used in prior research to manufacture silicon carbide nanofilms of polyvinyl alcohol. A substrate for spin coating with a 40 mm diameter was made of glass that

had been covered in aluminum foil. On the spin coating machine's base, the composite was then put. At 750 rpm, run for 10 seconds. Samples were prepared for the tests by being kept at room temperature for 6 days while being separated from the substrate.

2.3 Characterization

A UV-VIS spectrophotometer was used to measure the absorption spectrum of nanoscale silicon carbide solutions and films and common polyvinyl alcohol in the wavelength range of (190–1100) nm with a wavelength range of 6V 10W tungsten halogen lamp light source. Absorption, optical absorption coefficient, energy gap, Erbach energy, and extinction coefficient, are found FTIR spectroscopy was performed using an ABB spectrometer (MB 3000) in the range 4000–600 cm^{-1} . For the determination of functional groups and field emission scanning electron microscopy (FESEM) measurements, TESCAN-MIRA II LMH was used.

3. RESULTS AND DISCUSSION

3.1 FT-IR Measurement

Figure (1) illustrates a compound's molecular bonds and the FTIR test. For polyvinyl alcohols, functional groups are one of the major contributing factors to the nano polymers composite, and FTIR determines the presence of organic and inorganic molecular groups in the samples. Depending on the infrared absorption frequency range from (4000 to 600) cm^{-1} , Fourier infrared (FTIR) spectroscopy was used For the analysis of functional groups and molecular bonds in nanocomposites, the specific molecular groups present in the sample will be determined through spectrum data in the origin program, as in the Figure. The intensity of this band rises and divides into peaks after increasing the concentration of implanted nano silicon carbide nanoparticles showing an increase in dipole momentum resulting from the interaction between O–H groups in PVA and nano silicon carbide (Si–H, C–OH). Thus, it can be inferred that the silicon carbide nanofiller interacts with hydrogen and oxygen atoms of the PVA backbone chains [13][14]. PVA nanocomposite Polyvinyl alcohol (PVA) –SiC nanocomposites, The peak around 2313 cm^{-1} represents the $\text{C}\equiv\text{C}$ stretching, These vibrational peaks indicate the monomer structure of PVA. Peak related to the stretching vibration of O–H shift from 3335 cm^{-1} to 3714 cm^{-1} in polymer nanocomposite films due to the reaction between PVA and SiC nano crystal stretching vibration shift from 3714 cm^{-1} lower wavenumber in PVA 3335 cm^{-1} Take note that the peak around in the nanocomposite film 3353 cm^{-1} represents a $\text{C}\equiv\text{H}$ stretching and the resulting C–H stretching vibration peak is from 2979 cm^{-1} PVA to 2923 cm^{-1} in the nanocomposite film in the literature [15] [13]. For PVA and PVA-SiC nanocomposites, the PVA sample showed spectrum peaks of 3714 cm^{-1} and 2923 cm^{-1} They are thought to be brought on by the flexing vibrations of the O–H respectively, C–H bonds. Its peaks at 1729 cm^{-1} and 1245 cm^{-1} are attributed to vibration and bond stretching C=O and C–O double due to the residual acetyl group found in PVA, and single, respectively, Peak vibration occurs at 1417 cm^{-1} are assigned to the flexural and stretching modes of C–H in PVA structure while the peaks at 1056 cm^{-1} are assigned to the Si–O–C stretching vibrations in the literature [15] [16]. It is noted that the peak slightly



developed. Table (2) shows the direct and indirect energy gap values and the Urbach energy. matrix has developed.

To calculate the **absorption coefficient** using equation (3)[24]:

$$\alpha = 2.303 \left(\frac{A}{t} \right) \dots\dots\dots(3)$$

Where: α the absorption coefficient and A the absorbance are the t thickness of the cheat. Figure (5) shows the absorption coefficient at wavelengths the absorption coefficient was calculated the reason is that the amount of optical absorption begins the integration of nanocrystals in the PVA matrix has decreased the distance between HOMO and LUMO levels [25]. This increased the process of electronic transitions with lower energies between the equivalence band(HOMO) and the level of impurities as well as the usual transitions between energy packs, and thus increased the process of optical absorption of the incident rays, which caused a rapid increase in the value of the coefficient of Absorption the results indicated a significant enhancement in absorption coefficient up to 22.5 %, 27.1%,29%, and 45% with increasing the contribution of silicon carbide concentrations in the nanocomposites up to(0%,0.90, 0.93, and 0.95)wt %, respectively. As for the sample (s_3) against (0.91%) wt, we notice a decrease in the values of the absorbance coefficient 24.5% due to the decrease in the granular size and the increase in the granular boundaries, which led to the heterogeneity of the material[65]. The maximum absorbance coefficient at the wavelength range is 200 nm as long as we see that the absorbance coefficient increases with the increase in the concentration of silicon carbide nanoparticles in polyvinyl alcohol the transitions are found to be $\pi \rightarrow \pi^*$, The transition $n \rightarrow \pi^*$ is discovered when the wavelength of all ratios is increased up to 230 nm .

The extinction coefficient is calculated from the relationship [26].

$$K = \alpha\lambda/4\pi \dots\dots\dots(4)$$

The extinction coefficient refers to the amount of attenuation that an electromagnetic wave gets when it passes through a material medium, and on this basis, its amount is determined by the interaction of the electromagnetic wave with the medium, where the fading coefficient was calculated as From the equation (4) as in Figure (6) that the extinction coefficient k , in general, is similar to the nature of the curves almost the absorption coefficient curves, the results indicated a significant enhancement in extinction coefficient up to 13.2 %, 17%,18.4%, and 23. % with increasing the contribution of silicon carbide concentrations in the nanocomposites up to(0%,0.90, 0.93, and 0.95)wt %, respectively. As for the sample (s_3) against (0.91%) wt, we notice a decrease in the values of the extinction coefficient 15% due to the decrease in the granular size and the increase in the granular boundaries, which led to the heterogeneity of the of doping and the reason for this is that Impurities built new levels within the energy gap, which increased the absorption coefficient and decreased the wavelength, and thus the optical energy gap decreases as a result of absorption[21][27].



3.3 Field emission electron microscopy

used to show the morphology of the samples. Typical images showing and describing the formation and dispersion of SiC nanoparticles with different amounts by weight in polymer chains respectively . It is well known that SiC some particles have a strong tendency to agglomerate due to the presence of a strong interaction force between them and the surface tensile agent of the polymer as well [28]. Despite the gradual growth of the proportion of nanoparticles in polymer mixtures, the surface shape changes. The small, distinct polyvinyl alcohol chains are spherical, come in a variety of diameters, and some of the bigger chains include tiny very small pores inside the structure the field's imaging resolution was 200 nm. The FESEM test show that films are composite nano and particle size will increase except one sample will be decreased, the magnification is 200nm. In the first sample (s_1) as in Figure (7), the surface is clarified in pure PVA film, which indicates the smoothness of the surface. Since no filler is added to the polyvinyl alcohol, therefore, there is no difference in the PVA polymer surfaces. , PVA appeared to be homogeneous and the grain size was 317 nm. Then there will be a noticeable change in the structure of (pure) PVA after adding SiC which can be seen in the Figures successively. In the sample (s_2) as in Fig. (8), the grain size decreased to 33 nm. This means that there is a silicon carbide nanoparticles with a polyvinyl alcohol copolymer. And in sample (s_3) as in Figure (9), the size of the granules was (30 nm) and this means that the sizes of the granules decreased, then in the sample (S_4) as in Figure (10) the size and size of the granules increased (42 nm) and in The sample (S_5) as in Figure (11) has increased in size (56 nm), and this means that the third sample has the lowest particle size and thus means an increase in the granular boundaries within the material (PVA) and there is also an agglomeration of SiC particles in PVA, the bonding between the two surfaces becomes Carbide and polymer material are weak, which increases the elongation in its mechanical properties in addition to decrease the conductivity [29].

Table (1). Materials are weighed using a sensitive scale

NO Sample	PVA		Nano sic Wt%	Total weight fraction
	Wt%	Weight gm		
1	100%	0.8	0%	100%
2	99.10%	0.79	0.90%	100%
3	99.09%	0.78	0.91%	100%
4	99.07%	0.77	0.93%	100%
5	99.05%	0.76	0.95%	100%

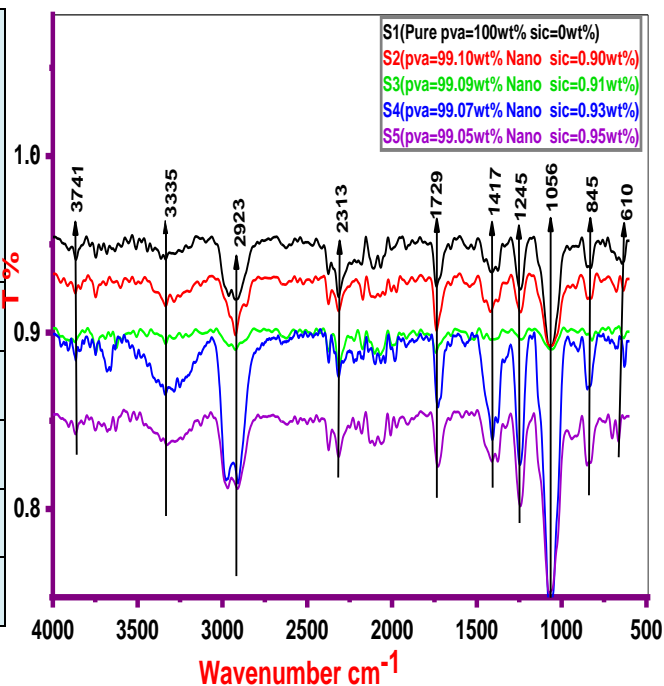


Figure 1: FTIR

Table (2) shows the values of the direct and indirect energy gap and Urbach energy)

PVA		Nano SiC Wt%	Total weight fraction	Direct Energy Gap (eV)	Indirect energy gap (eV)	Urbach energy (eV)
Wt%	Weight gm					
100%	0.8	0%	100%	5.585	5.006	2.38
99.10%	0.79	0.90%	100%	5.310	4.880	2.45
99.09%	0.78	0.91%	100%	5.480	4.916	2.94
99.07%	0.77	0.93%	100%	4.986	4.683	2.74
99.05%	0.76	0.95%	100%	4.800	4.490	3.67

مجله علمی پژوهشی فصلنامه علمی پژوهشی فصلنامه علمی پژوهشی فصلنامه علمی پژوهشی فصلنامه علمی پژوهشی

ISSN: 2312-8135 | Print ISSN: 1992-0652 | info@journalofbabylon.com | jub@itnet.uobabylon.edu.iq | www.journalofbabylon.com



تعمیر و بازسازی و احیای بناهای تاریخی و فرهنگی و مرمت و نگهداری از آثار و بناهای تاریخی و فرهنگی و مرمت و نگهداری از آثار و بناهای تاریخی و فرهنگی

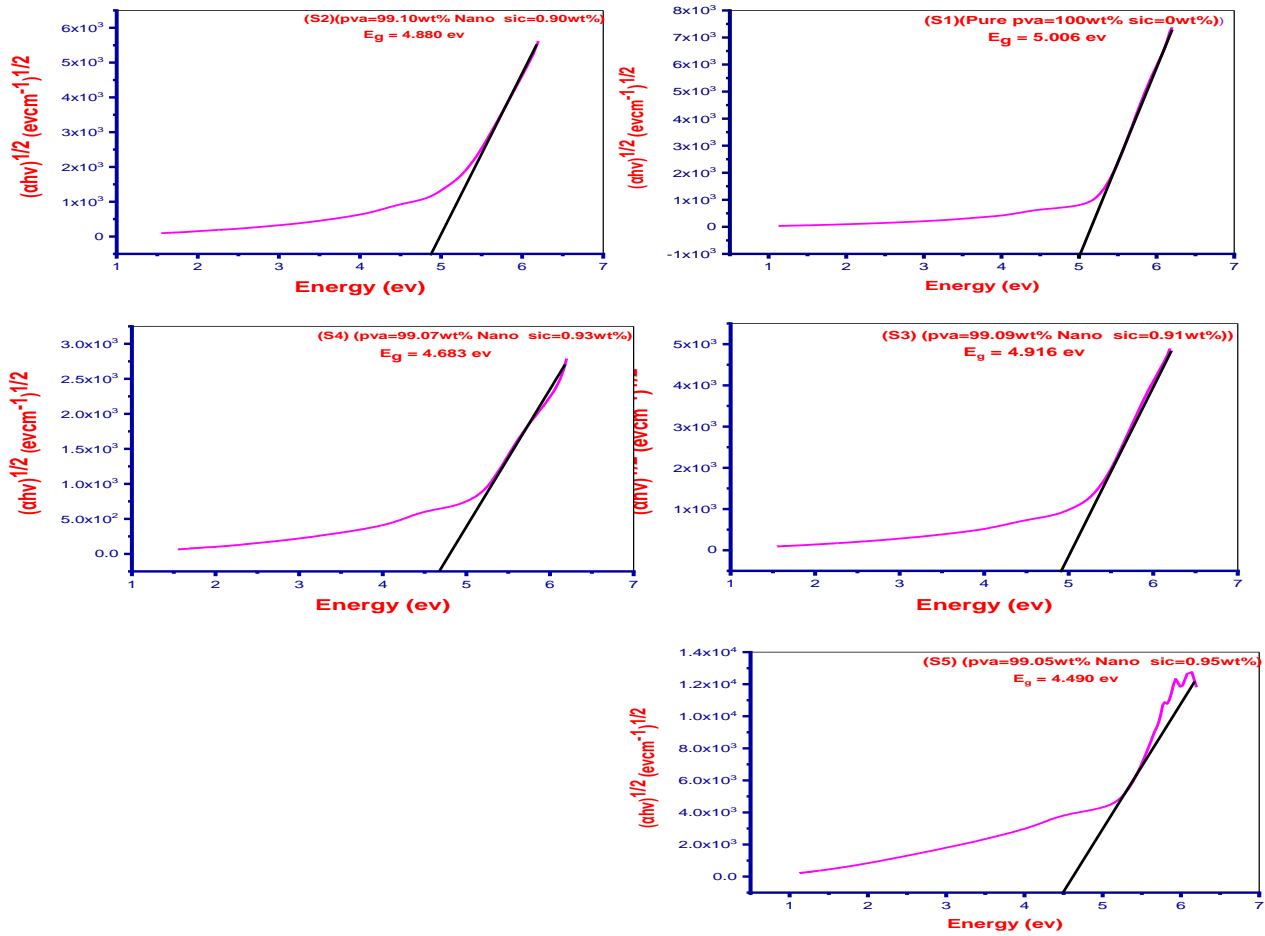


Figure (2) shows the indirect optical energy.



مبدئيًا، يتم تصنيع الأغشية الرقيقة باستخدام طريقة التبخير الحراري في جو فراغ. يتم تحضير الأغشية الرقيقة من مادة البولي (بيفلافونيك أسيد) باستخدام طريقة التبخير الحراري في جو فراغ. يتم تحضير الأغشية الرقيقة من مادة البولي (بيفلافونيك أسيد) باستخدام طريقة التبخير الحراري في جو فراغ.

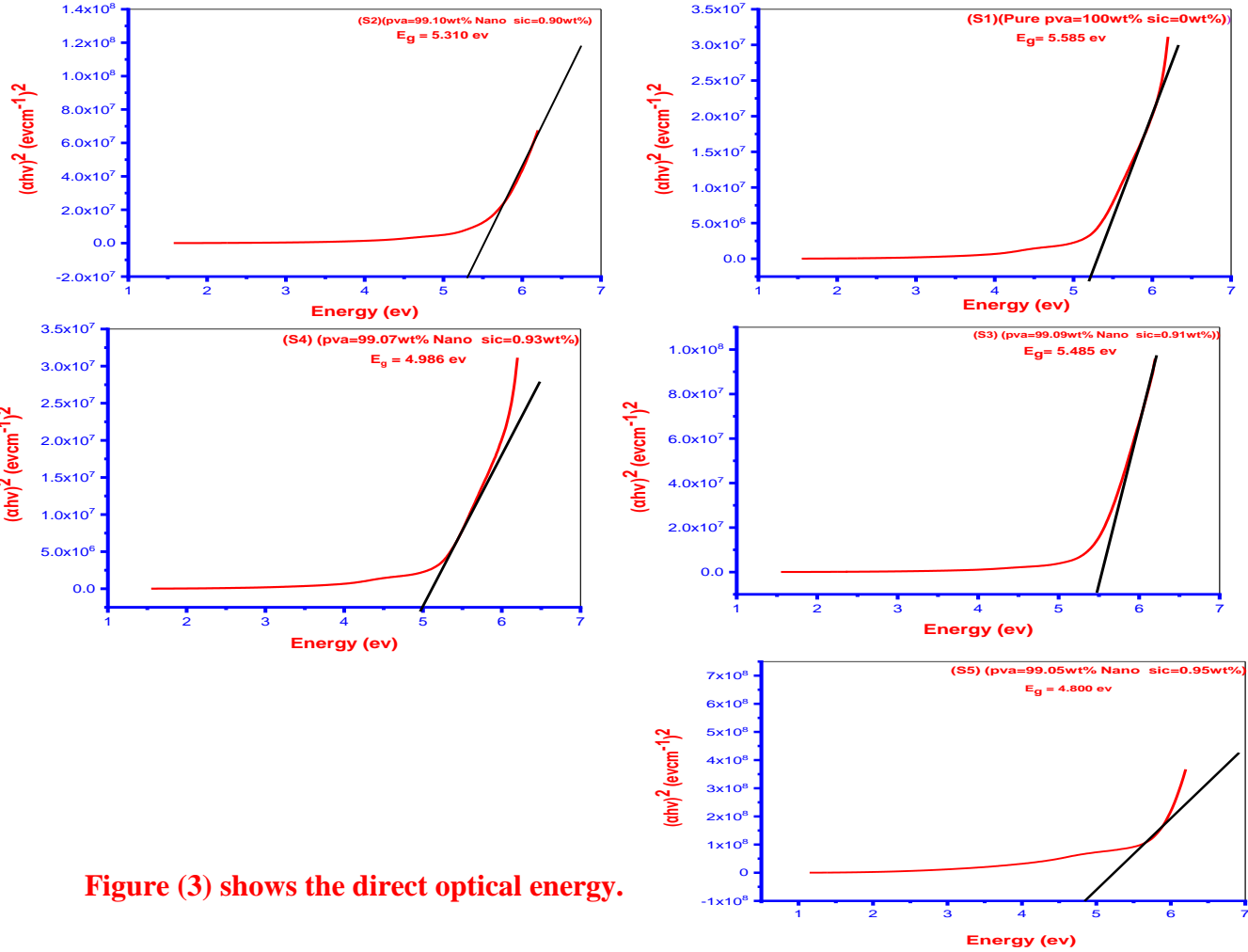


Figure (3) shows the direct optical energy.

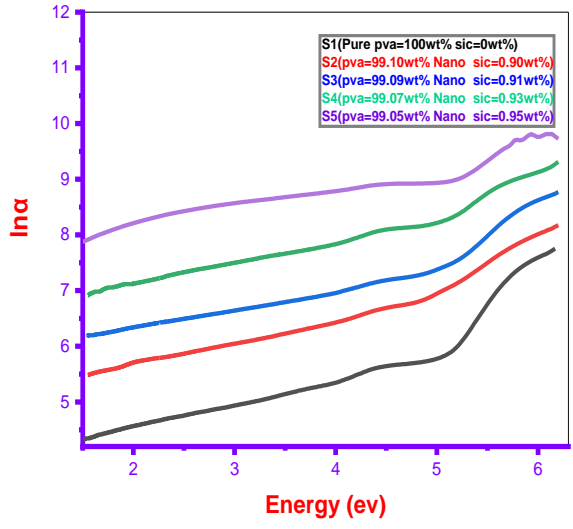
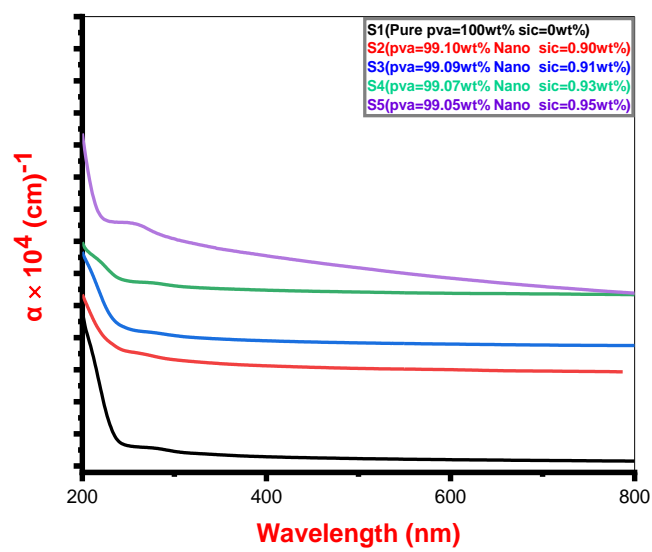


Figure (4) Shows Urbach energy



Figure(5) Shows the Absorbance Coefficient at Wavelengths.

ISSN: 2312-8135 | Print ISSN: 1992-0652
 info@journalofbabylon.com | jub@itnet.uobabylon.edu.iq | www.journalofbabylon.com

مجلة جامعة بابل للعلوم التطبيقية و التكنولوجية | المجلد 31، العدد 3، 2023 | ISSN: 1992-0652

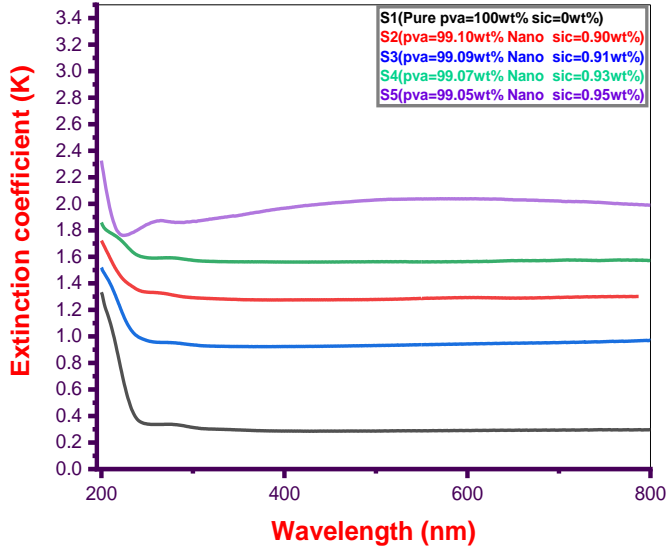


Figure (6) Extinction coefficient at Wavelength.

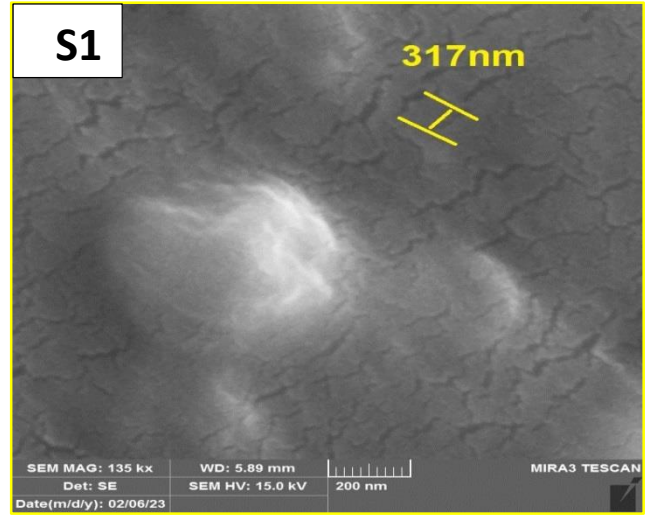


Figure (7) SEM micrograph PVA =100wt%)

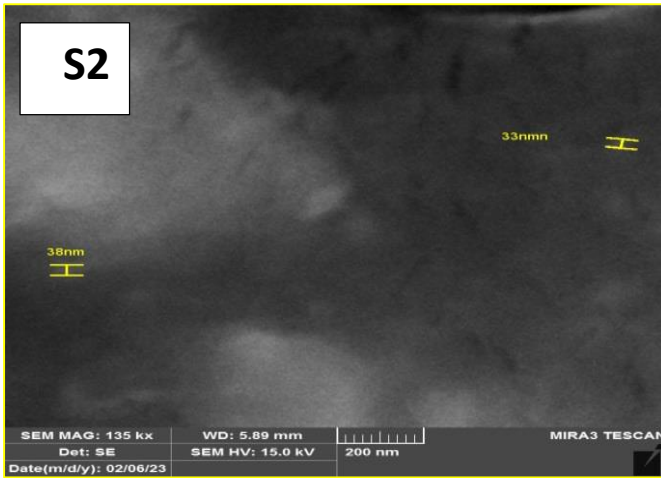


Figure (8) FESEM micrograph of sample (PVA =99.10wt% Nano SiC=0.90wt %)

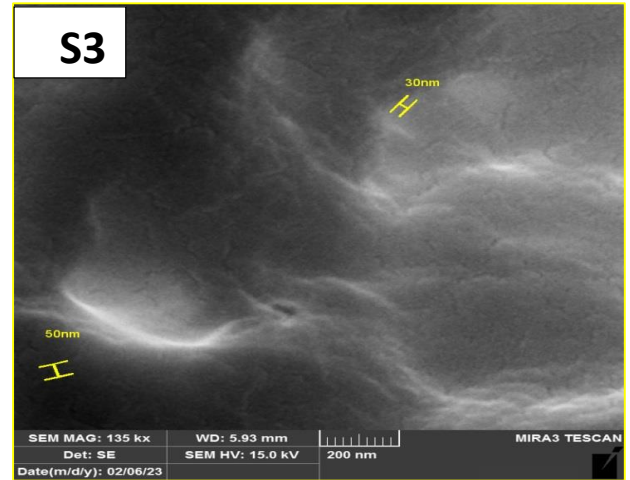


Figure (9) FESEM micrograph of sample (PVA =99.09wt% Nano SiC=0.91wt %)

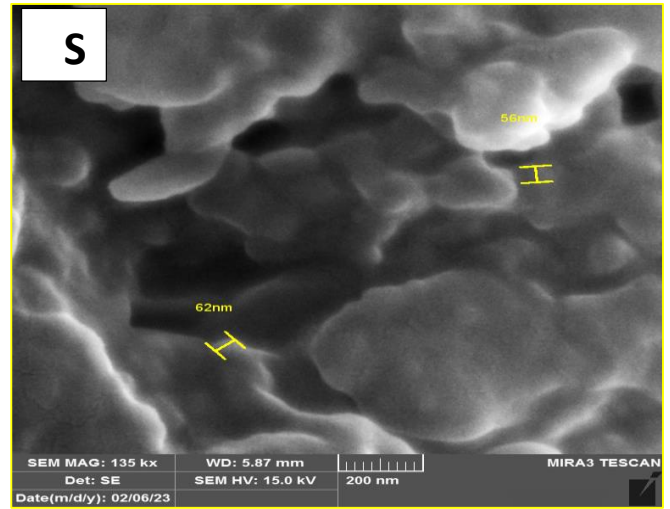
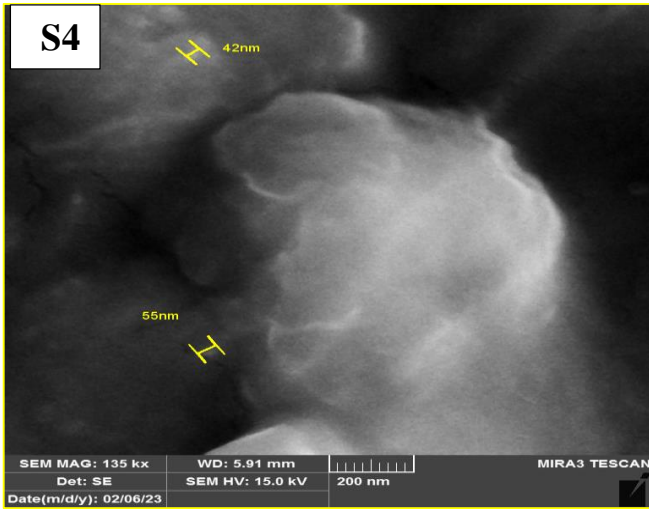


Figure (10) FESEM micrograph of sample (PVA =99.07wt% Nano SiC=0.93wt%) **Figure (11) FESEM micrograph of sample (PVA=99.05wt% Nano SiC=0.95wt%)**

5. CONCLUSION

The sic-PVA polymeric nanocomposites were manufactured by adding silicon carbide nanoparticles extracted by pulsed laser to polyvinyl alcohol pva, and the FTIR examination was performed to find out the functional groups and the bonding of the bonds between the atoms, and the interaction between them, it was found that the reaction was Physical, not chemical, because no new bonds appeared or bonds disappeared, and the evidence for that interaction is Physical, FT-IR spectra show a shift in some bands and a change in the intensities of other bands compared with pure poly-blend films. and the FESEM examination was performed, and an improvement was shown in the distribution of nanoparticles in general in the polymer pva. Absorbance, the absorption coefficient, the extinction coefficient, increased with increasing weight percentages of silicon carbide nanoparticles with a slight decrease at SiC = 0.91 wt%. The optical energy gaps and the Urbach energy decrease with increasing SiC nanomaterials concentrations and the energy gap increases slightly at SiC 0.91 wt%) it results showed an improvement in the optical properties after adding nanoscale silicon carbide .



Conflict of interests

There are non-conflicts of interest.

References

- [1] Y.-Y. Yu, W.-C. Chien, and S.-Y. Chen, "Preparation and optical properties of organic/inorganic nanocomposite materials by UV curing process," *Mater. Des.*, vol. 31, no. 4, pp. 2061–2070, 2010.
- [2] S. S. Hegde, A. G. Kunjomana, K. A. Chandrasekharan, K. Ramesh, and M. Prashantha, "Optical and electrical properties of SnS semiconductor crystals grown by physical vapor deposition technique," *Phys. B Condens. Matter*, vol. 406, no. 5, pp. 1143–1148, 2011.
- [3] V. Chaudhary, A. K. Thakur, and A. K. Bhowmick, "Improved optical and electrical response in metal–polymer nanocomposites for photovoltaic applications," *J. Mater. Sci.*, vol. 46, pp. 6096–6105, 2011.
- [4] S. Jeong, H. Choi, J. Y. Kim, and T. Lee, "Silver-based nanoparticles for surface plasmon resonance in organic optoelectronics," *Part. Part. Syst. Charact.*, vol. 32, no. 2, pp. 164–175, 2015.
- [5] J. Xu, K. Wang, S.-Z. Zu, B.-H. Han, and Z. Wei, "Hierarchical nanocomposites of polyaniline nanowire arrays on graphene oxide sheets with synergistic effect for energy storage," *ACS Nano*, vol. 4, no. 9, pp. 5019–5026, 2010.
- [6] M. Moussa, M. F. El-Kady, Z. Zhao, P. Majewski, and J. Ma, "Recent progress and performance evaluation for polyaniline/graphene nanocomposites as supercapacitor electrodes," *Nanotechnology*, vol. 27, no. 44, p. 442001, 2016.
- [7] H. Gu *et al.*, "Flame-retardant epoxy resin nanocomposites reinforced with polyaniline-stabilized silica nanoparticles," *Ind. Eng. Chem. Res.*, vol. 52, no. 23, pp. 7718–7728, 2013.
- [8] M. E. Marques, A. A. P. Mansur, and H. S. Mansur, "Chemical functionalization of surfaces for building three-dimensional engineered biosensors," *Appl. Surf. Sci.*, vol. 275, pp. 347–360, 2013.
- [9] I. Saini, A. Sharma, J. Rozra, R. Dhiman, S. Aggarwal, and P. K. Sharma, "Modification of structural, thermal, and electrical properties of PVA by addition of silicon carbide nanocrystals," *J. Appl. Polym. Sci.*, vol. 132, no. 34, 2015.
- [10] J. Cao, J. Zhao, X. Zhao, G. Hu, and Z. Dang, "Preparation and characterization of surface modified silicon carbide/polystyrene nanocomposites," *J. Appl. Polym. Sci.*, vol. 130, no. 1, pp. 638–644, 2013.
- [11] D. Coetsee, M. Venkataraman, J. Militky, and M. Petru, "Influence of nanoparticles on thermal and electrical conductivity of composites," *Polymers (Basel)*, vol. 12, no. 4, p. 742, 2020.
- [12] I. Saini, A. Sharma, R. Dhiman, S. Aggarwal, S. Ram, and P. K. Sharma, "Grafted SiC nanocrystals: For enhanced optical, electrical and mechanical properties of polyvinyl alcohol," *J. Alloys Compd.*, vol. 714, pp. 172–180, 2017, doi: 10.1016/j.jallcom.2017.04.183.
- [13] R. A. Hadhy and B. Y. Kadem, "Gel Polymer Electrolyte Based on SiC: PVA Composites for Body Motion Sensor and Paper Based Application," in *2019 12th International Conference on Developments in eSystems Engineering (DeSE)*, 2019, pp. 730–735.
- [14] S. Mahendia, A. K. Tomar, R. P. Chahal, P. Goyal, and S. Kumar, "Optical and structural



- properties of poly (vinyl alcohol) films embedded with citrate-stabilized gold nanoparticles," *J. Phys. D. Appl. Phys.*, vol. 44, no. 20, p. 205105, 2011.
- [15] O. W. Guirguis and M. T. H. Moselhey, "Optical study of poly (vinyl alcohol)/hydroxypropyl methylcellulose blends," *J. Mater. Sci.*, vol. 46, pp. 5775–5789, 2011.
- [16] B. Stuart, *INFRARED SPECTROSCOPY : FUNDAMENTALS AND*, vol. 8. 2004.
- [17] J. P. Li *et al.*, "Structural characterization of nanometer SiC films grown on Si," *Appl. Phys. Lett.*, vol. 62, no. 24, pp. 3135–3137, 1993.
- [18] M. H. AL-humairi, "Study the optical and electrical properties of (PVA-Ag) and (PVA-TiO₂) Nanocomposites." M. Sc. Thesis, University of Babylon, College of Education for Pure Sciences, 2013.
- [19] R. S. Kundu and S. Dhankhar, "R. punia, K. Nanda, N. Kishore," *Bismuth Modif. Phys. Struct. Opt. Prop. mid-IR transparent zinc boro-tellurite Glas. J. Alloy. Comp*, vol. 587, pp. 66–73, 2014.
- [20] C.-J. He *et al.*, "Orientation effects on the bandgap and dispersion behavior of 0.91 Pb (Zn_{1/3}Nb_{2/3}) O₃-0.09 PbTiO₃ single crystals," *Chinese Phys. B*, vol. 21, no. 5, p. 54207, 2012.
- [21] G. Kaur, R. Adhikari, P. Cass, M. Bown, and P. Gunatillake, "Electrically conductive polymers and composites for biomedical applications," *Rsc Adv.*, vol. 5, no. 47, pp. 37553–37567, 2015.
- [22] R. N. Abed *et al.*, "Optical and morphological properties of poly (vinyl chloride)-nano-chitosan composites doped with TiO₂ and Cr₂O₃ nanoparticles and their potential for solar energy applications," *Chem. Pap.*, vol. 77, no. 2, pp. 757–769, 2023.
- [23] M. M. Kamble *et al.*, "Prepared with High Deposition Rate by Hot Wire Chemical Vapor Deposition Method," *J. Coatings*, vol. 2014, no. ID 905903, pp. 1–11, 2014, [Online]. Available: <http://www.hindawi.com/journals/jcoat/2014/905903/>
- [24] R. Sahebi, "Comment on:'Optical study on single-layer photoluminescent graphene oxide nanosheets through a simple and green hydrothermal method'[J. Photochem. Photobiol. A Chem. 364 (2018) 595–601]," *J. Photochem. Photobiol. A Chem.*, vol. 401, p. 112750, 2020.
- [25] I. Saini, A. Sharma, R. Dhiman, S. Aggarwal, S. Ram, and P. K. Sharma, "AC," *J. Alloys Compd.*, 2017, doi: 10.1016/j.jallcom.2017.04.183.
- [26] S. A. Tawfiq, "A study of optical and electrical properties of the cadmium stannate material using the Co-Evaporation method," *Phyther. Res.*, vol. 57, pp. 1257–1274, 1996.
- [27] W. S. Khan, N. N. Hamadneh, and W. A. Khan, "Polymer nanocomposites–synthesis techniques, classification and properties," *Sci. Appl. Tailored Nanostructures*, vol. 50, 2016.
- [28] D. Pinto, L. Bernardo, A. Amaro, and S. Lopes, "Mechanical properties of epoxy nanocomposites using titanium dioxide as reinforcement–a review," *Constr. Build. Mater.*, vol. 95, pp. 506–524, 2015.
- [29] N. Bisht, A. Verma, S. Chauhan, and V. K. Singh, "Effect of functionalized silicon carbide nanoparticles as additive in cross-linked PVA based composites for vibration damping application," *J. Vinyl Addit. Technol.*, vol. 27, no. 4, pp. 920–932, 2021, doi: 10.1002/vnl.21865.

الخلاصة

المقدمة: يُعتقد أن تعزيز الخصائص البصرية لأغشية كحول البولي فينيل النانوية وكربيد السيليكون أمر بالغ الأهمية للحصول على أشباه الموصلات بأقل فجوة طاقة للتطبيقات في الأجهزة الكهربائية والشاشات الرقمية وأجهزة الاستشعار.

طرق العمل: تم فحص الخصائص البصرية لكحول الفينيل وكربيد السيليكون. يتم استخدام الليزر النبضي بطول موجي 532 نانومتر لإنشاء هذه الجسيمات النانوية إلى جسيمات نانوية واسعة الانتشار في بيئتين (الماء وكحول الفينيل). تم إنشاء مركب نانوي كحول عديد الفينيل بواسطة جزيئات كربيد السيليكون المغلفة بالدوران مع النسب الوزنية 0.90% ، 0.91% ، 0.93% ، و 0.95%. تم استخدام مطيافية فورييه لتحديد المجموعات الوظيفية القائمة. تم استخدام تقنيات FESEM لتحليل تكوين السطح وتشتت الجسيمات النانوية على سطح غشاء المركب النانوي. باستخدام التحليل الطيفي UV-Vis المستخدم لتسجيل طيف الامتصاص في نطاق (200-800) نانومتر للأشعة فوق البنفسجية.

النتائج: تم حساب فجوة الطاقة المباشرة (4.800, 4.986, 5.480, 5.310, 5.585) إلكترون-فولت وغير المباشرة (5.006, 4.490, 4.683, 4.916, 4.880) إلكترون-فولت وطاقة اورياخ (3.67, 2.74, 2.94, 2.45, 2.38) إلكترون-فولت للعينات بنسبة والامتصاصية ومعامل الامتصاص ومعامل الخمود كما في الجدول رقم 1 على التوالي.

الاستنتاجات: من خلال التحقيق في الخصائص البصرية للجسيمات النانوية ، مثل معاملات الانقراض والامتصاص ، وفجوات الطاقة الضوئية المباشرة وغير المباشرة ، وطاقات Urbach. زيادة في الانقراض ومعاملات الامتصاص طاقة Urbach عند إضافة كربيد النانو إلى كحول البولي فينيل ، تظهر النتائج تضييقاً مباشراً و فجوات الطاقة غير المباشرة. هذا يشير إلى أن الخصائص البصرية للمركب النانوي قد تحسنت.

الكلمات المفتاحية

مركبات النانو بولي فينيل الكحول، كربيد السيليكون ، الأشعة فوق البنفسجية، مطيافية فورييه.